Two-wavelength holographic interferometer

Philip Lam, J. D. Gaskill, and James C. Wyant

It has been demonstrated that a $Bi_{12}SiO_{20}$ crystal is a good holographic recording medium. Using this crystal as a real-time recording device, a two-wavelength holographic interferometer has been constructed. The 488- and 514.5-nm lines of an Ar-ion laser were used as the source to yield an equivalent wavelength of 9.47 μm.

I. Introduction

In optical testing, when the wave-front error of a test optic is much larger than the wavelength of visible light, it may be difficult to analyze the closely spaced interference fringes in the interferogram. The use of a less-sensitive testing technique or a long-wavelength interferometer would be preferred for this purpose. In addition, when the optic is to be tested in transmission, the wavelength that can be used in the interferometer is further restricted by the transmission range of the test piece. In this and other applications, two-wavelength holographic contouring[1-3] is convenient and appropriate.

II. Construction of the Two-Wavelength Holographic Interferometer

In two-wavelength holographic contouring, a hologram of the test wave front is made using the first wavelength, while the reconstruction is obtained using the second wavelength. The resulting interference between the wave front coming from the test optic and the reconstructed wave front from the hologram gives an interferogram of the test optic at the second wavelength.

The interferogram is interpreted using an equivalent wavelength

$$\lambda_{eq} = \frac{\lambda_1 \lambda_2}{|\lambda_1 - \lambda_2|},$$

where λ_1 is used to make the hologram, and λ_2 is used in the reconstruction.

A two-wavelength holographic interferometer has been constructed using a BSO crystal as the holographic recording medium. The crystal works in real time, is reusable, and eliminates the need for film and processing. This makes the instrument excellent for routine contouring. The interferometer is shown in Fig. 1. The two wavelengths of 488 nm (blue) and 514.5 nm (green) of a single-mode Ar-ion laser are used as the source. The crystal has dimensions of 10 × 10 × 3.1 mm, is biased along the [110] direction between 4 and 6 kV, and is used in the standard crystallographic orientation.[4]

As shown in the figure, the light from the laser source is divided into the upper and lower arms of the interferometer by a variable beam splitter. In the upper arm, after the 45° right-angle prism, the green collimated wave serves as the reference wave, while the blue collimated wave serves as the reconstruction wave. One deviates from the other by a small angle Δ. The collimated waves going through the test optic in the lower arm are the green test wave and the blue test wave. Preceding the collimator in the test arm, a long-pass edge filter passes most of the green wavelength but passes only a fraction of a percent of the blue wavelength.

In the actual setup, two commercially available edge filters were used instead of a single custom-made edge filter. Each of the two filters was tilted at the appropriate angle to pass the right amount of light for each of the two wavelengths. The variable beam splitter at the left was adjusted so that the green interference pattern would attain the best visibility at the crystal. At this intensity ratio the blue interference pattern had poor contrast. Thus a good hologram was formed only at the green wavelength in the 3.1-mm thick crystal.

To reconstruct the test wave front in the blue wavelength from this thick phase hologram, Bragg's condition had to be observed.[5] A narrowband interference filter was placed after the crystal to pass only the blue test wave and the blue reconstructed wave. Because
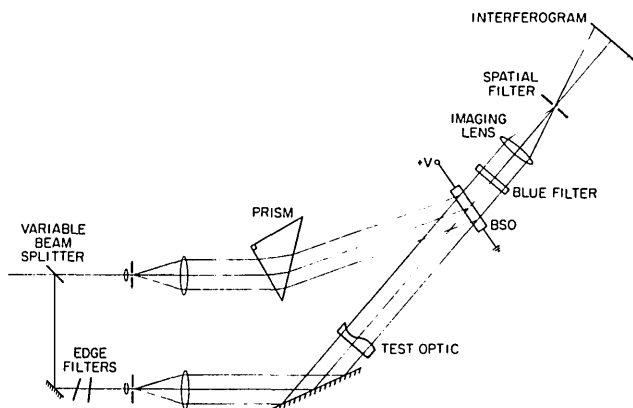
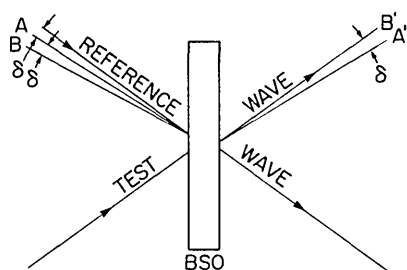Fig. 1. Configuration of two-wavelength holographic interferometer.

Fig. 2. Direction of reconstructed wave. A and B are the reconstruction waves. A' and B' are the respective reconstructed waves. A is at Bragg's incidence.

Fig. 3. ϕ is the angle of incidence at the prism. Δ is the angular deviation of the blue light from the green light.

of its low intensity, the blue interferogram formed after the imaging lens was degraded by the light scattered from different components of the system. Spatial filtering[6] was found effective for filtering out the noise in the interferogram.

The prism in the upper arm serves two purposes, one of which is to deal with the Bragg requirement. After passing through the prism, the deviation of the blue wave from the green wave will satisfy Bragg's condition for one spatial frequency of the hologram. To match this frequency, the angle between the reference wave and the green test wave was set appropriately. However, at the Bragg incidence, the blue reconstructed wave does not propagate at the same angle as the blue test wave as shown in Fig. 2. As a result, a large number of tilt interference fringes are present in the interferogram. Let δ be the deviation angle necessary to satisfy Bragg's law; only when the reconstruction wave deviates from the reference wave by 2δ will the reconstructed wave align with the test wave. At this angle, the diffraction efficiency of the blue reconstruction is low because of detuning from the Bragg angle.

In addition to the need for high intensity at the interferogram, a way must be provided in the interferometer to control the amplitudes of the blue waves to give good interference fringes. The amplitude of the blue reconstructed wave can be varied by adjusting the crystal bias voltage, while the amplitude of the blue test
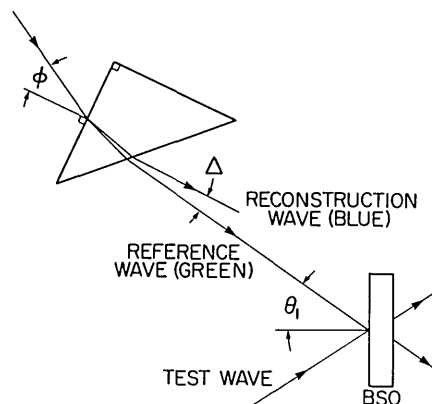
wave can be tuned by the long-pass edge filter. To obtain a blue interferogram of high visibility, these two amplitudes have to be closely matched.

The other purpose of the prism is to introduce the desired amount of tilt in the interferometer. The amount of tilt is controlled by turning the prism. It functions as follows: The 45° right-angle prism has a refractive index of 1.652 at the wavelength of 514.5 nm and 1.657 at 488 nm. Referring to Fig. 3, the deviation angle Δ of the blue wave from the green wave can be written as a function of the incident angle ϕ,

$$\Delta = \sin^{-1}\left\{1.657 \sin\left[45 - \sin^{-1}\left(\frac{\sin\phi}{1.657}\right)\right]\right\}$$
$$- \sin^{-1}\left\{1.652 \sin\left[45 - \sin^{-1}\left(\frac{\sin\phi}{1.652}\right)\right]\right\}.$$

For Bragg's condition

$$\frac{\sin\theta_1}{\lambda_1} = \frac{\sin\theta_2}{\lambda_2},$$

$$\delta = \theta_1 - \theta_2 = \theta_1 - \sin^{-1}\left[\frac{488}{514.5}\sin\theta_1\right].$$

When the prism turns, ϕ, θ_1, and δ change. There are no tilt interference fringes when Δ is equal to 2δ. Curves were plotted for Δ and 2δ against ϕ in Fig. 4.
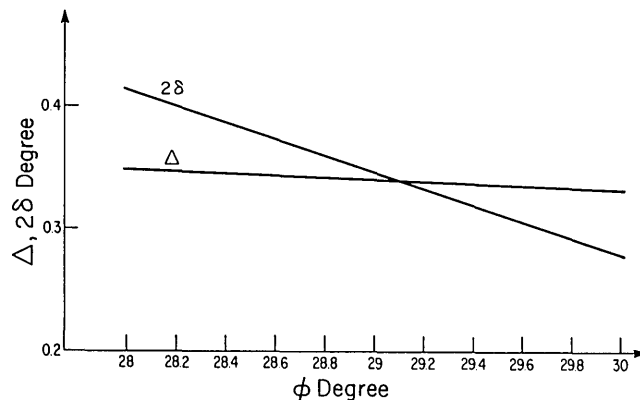

Fig. 4. Under- and over-match of Δ with 2δ. In this example, θ_1 is 3.25° when Δ equals 2δ.
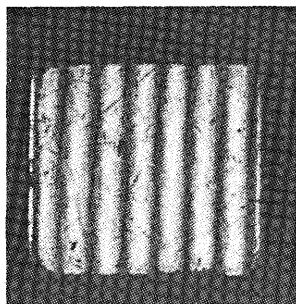
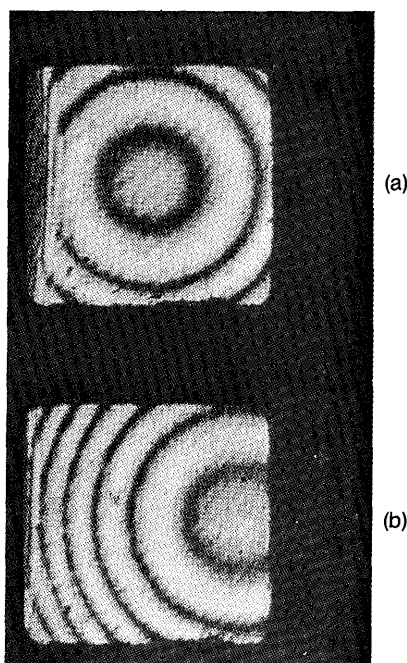Fig. 5. Interferometer with no test optic; $\lambda_{eq} = 9.47 \, \mu m$.

(a)

(b)

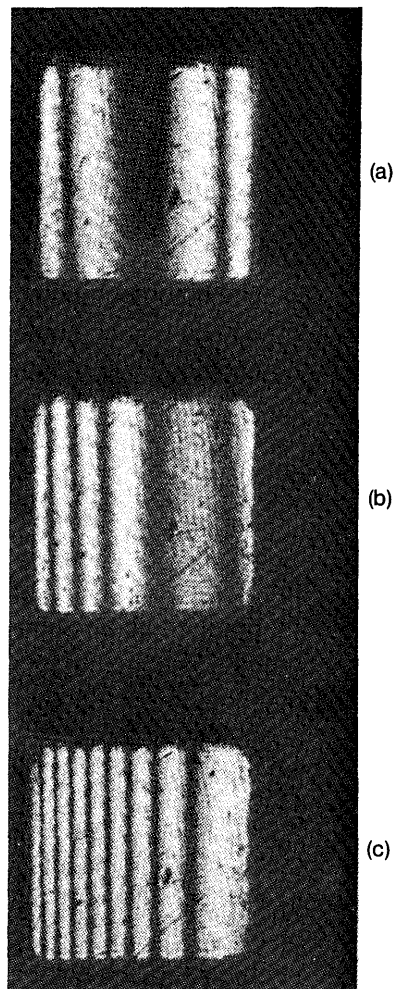Fig. 6. Spherical concave ophthalmic lens: (a) no tilt; (b) small amount of tilt.

(a)

(b)

(c)

Fig. 7. Cylindrical concave ophthalmic lens: (a) no tilt; (b) small amount of tilt; (c) large amount of tilt.

Over the range of a 2° change in ϕ, the change in Δ is slow, whereas the change in 2δ is rapid. The under match and the over match of Δ to 2δ introduces the desired amount of tilt in the interferogram.

III. Conclusion

The interferometer described in this paper works well. Figure 5 shows an interferogram formed with no test optic. Figures 6 and 7 show the interferograms of two ophthalmic lenses. In the present configuration of the interferometer, the dimensions of the test optic are limited by the aperture of the crystal. Since the crystal is sensitive to both the green and the blue wavelengths, the hologram reconstruction process is destructive. The construction of the hologram in the green wavelength and the reconstruction in the blue wavelength are simultaneous; thus the diffraction efficiency is reduced due to the destructive reconstruction. The temporal response and diffraction efficiency of the crystal are governed by the beam intensities, fringe spatial frequency, and the bias voltage.[7,8]

References

1. D. Malacara, *Optical Shop Testing* (Wiley-Interscience, New York, 1978).
2. S. S. Lam, Chris L. Koliopoulos, and J. C. Wyant, "Optical Metrology with Two-Wavelength Real-Time Holography," J. Opt. Soc. Am. **70**, 1591 (1980).
3. F. M. Küchel and H. J. Tiziani, "Real-Time Contour Holography Using BSO Crystals," Opt. Commun. **38**, 17 (1981).
4. J. P. Herrian, J. P. Huignard, and P. Aubourg, "Some Polarization Properties of Volume Hologram in $Bi_{12}SiO_{20}$ Crystals and Application," Appl. Opt. **17**, 1851 (1978).
5. R. J. Collier, C. B. Burckhardt, and L. H. Lin, *Optical Holography* (Academic, New York, 1971).
6. J. D. Gaskill, *Linear Systems, Fourier Transform, and Optics* (Wiley, New York, 1978).
7. J. P. Huignard, J. P. Herrian, and G. Rivet, "Phase-Conjugation and Spatial-Frequency Dependence of Wavefront Reflectivity in $Bi_{12}SiO_{20}$ Crystals," Opt. Lett. **5**, 102 (1980).
8. J. D. Gaskill, P. Lam, and J. C. Wyant, "Dependence of the Diffraction Efficiency of $Bi_{12}SiO_{20}$ on Recording Parameters," Proc. Soc. Photo-Opt. Instrum. Eng. **370**, 144 (1982).